

Planar Hall Resistance Sensor for Monitoring Current

KunWoo Kim¹, Sri Ramulu Torati², Venu Reddy², and SeokSoo Yoon^{1*}

¹*Department of Physics, Andong National University, Andong 760-749, Korea*

²*Department of Materials Science and Engineering, Chungnam National University, Daejeon 305-764, Korea*

(Received 28 March 2014, Received in final form 13 May 2014, Accepted 13 May 2014)

Recent years have seen an increasing range of planar Hall resistive (PHR) sensor applications in the field of magnetic sensing. This study describes a new application of the PHR sensor to monitor a current. Initially, thermal drift experiments of the PHR sensor are performed, to determine the accuracy of the PHR signal output. The results of the thermal drift experiments show that there is no considerable drift in the signals attained from 0.1, 0.5, 1 and 2 mA current. Consequently, the PHR sensor provides adequate accuracy of the signal output, to perform the current monitoring experiments. The performances of the PHR sensor with bilayer and trilayer structures are then tested. The minimum detectable currents of the PHR sensor using bilayer and trilayer structures are 0.51 μA and 54 nA, respectively. Therefore, the PHR sensor having trilayer structure is the better choice to detect ultra low current of few tens nanoampere.

Keywords : current sensor, Planar Hall Resistance (PHR), bilayer structure, trilayer structure

1. Introduction

Electric current measurement is a significant importance in many applications, including power, industrial, automobile and domestic applications. Various commonly used current sensors are available, and include shunt resistors, Rogowski coils, current transformers, Hall sensors, and fiber-optic current sensors [1-5]. These commercial sensors have many limitations; for example, shunt resistors are limited to use in high-current applications, due to high power losses; while Rogowski coils are not suitable for the measurement of low-frequency currents, as the output of the coil must be passed through an integrator circuit, and the practical integrator is not perfect, and shows some input off-set voltage [6]. Current transformers are similar to Rogowski coils, but in current transformers, the magnetizing inductance is not ideal, but shows some hysteresis and saturation [7]. Hall Effect sensors show high offset voltages and temperature effects, which ultimately influence the sensitivity of the sensor [8]. The fiber optic current sensor is expensive, and sometimes not useful for the measurement of small current [9]. Overall, almost all the sensing methods have some limitation for the measurement

of current. Hence, there is need to develop a sensor with high performance and good characteristics, for the measurement and monitoring of a current.

Magnetic current sensors, such as the Giant Magneto Resistance (GMR) and Anisotropic Magneto Resistance (AMR) sensor, have also been developed to measure electric current [10, 11]. However, the AMR and GMR magnetic current sensors have various weaknesses, including high thermal drift and non-linear behavior, which prevents their utility in current sensing applications. Recently, Planar Hall Resistive (PHR) magnetic sensors have proven their usefulness in various applications [12, 13]. PHR sensors are more sensitive and reliable than other sensors; and undesired effects, like non-linearity, hysteresis, saturation and thermal drift, can be avoided, by employing an appropriate technique [14]. These properties make the PHR sensor suitable for the measurement of current. Hence, we have developed a PHR-based magnetic current sensor.

In this paper, we fabricated PHR magnetic sensors with both bilayer and trilayer structure, and applied them for the measurement and monitoring of a current. The linearity of the output voltage versus applied current was measured for both bilayer and trilayer structure. The sensitivities of both types of sensors were calculated and compared, and the results showed that the trilayer structured sensor has higher sensitivity than the bilayer structure. The thermal drift and current response of the PHR sensors were mea-

©The Korean Magnetism Society. All rights reserved.

*Corresponding author: Tel: +82-54-820-5450

Fax: +82-54-823-1628, e-mail: yoon@andong.ac.kr

sured, to confirm their stability and resolution in current sensing.

2. Experimental Details

The PHR sensors of $50\ \mu\text{m} \times 50\ \mu\text{m}$, with either bilayer or trilayer structure, were patterned on a silicon wafer, using photo resist AZ 5214E (MicroChemicals, Germany), with conventional photolithography and lift-off technique. In brief, an active sensing junction of $50\ \mu\text{m} \times 50\ \mu\text{m}$ was stenciled on the photo resist, coated on the cleaned silicon substrate by developer, and rinsed with water. Both bilayer Ta(3 nm)/NiFe(10 nm)/IrMn(10 nm)/Ta(3 nm) and trilayer Ta(3 nm)/NiFe(10 nm)/Cu(1.2 nm)/IrMn(10 nm)/Ta(3 nm) structures were sputtered on the stenciled sensing junction of the silicon wafer, by DC magneto sputtering system, under a working pressure of 3 mTorr. A schematic of the layered structures is shown in Fig. 1(a). During the deposition process, a uniform magnetic field of 100 Oe was applied parallel to the film plane, to induce a magnetic anisotropy of ferromagnetic (FM) layers, and to align the pinning direction of the antiferromagnetic (AFM) IrMn layer, which fixed the easy axis of the sensor to the field direction. The photoresist was removed by a lift-off process, leaving the bilayer/trilayer sensing junction of $50\ \mu\text{m} \times 50\ \mu\text{m}$ structures on the silicon wafer substrate.

Electrodes of Ta (10 nm)/Au (150 nm) were fabricated to connect the sensor junction by a similar type of photolithography and lift-off process, and DC magnetron sputtering, for the measurement of electric circuitry. Subsequently, the sensor junctions and electrodes were passivated with a layer of SiO₂ of 150 nm thicknesses by RF magnetron sputtering, to protect the sensor junctions and electrodes from corrosion. The SiO₂ substrate containing both bilayer and trilayer sensors was attached to the PCB. The sensors and the PCB were connected, by using Au micro-wire bonding (7476D, West Bond Inc. USA), and the electrical connection was coated with epoxy, for protection from the environment. More details of the sensor fabrication process are described elsewhere [15]. A similar type of photolithography and the aforementioned lift-off process was used for the making of the current line (diagonally to the line), as shown in Fig. 1(b). The current line was $50\ \mu\text{m}$ wide and 200 nm thick. The measured current was applied along the line. The measured current produces a magnetic field on the PHR sensor, as shown in Fig. 1(c), and develops PHR voltage between the electrodes of +V and –V, when the driving current flows between the electrodes of +I and –I, as shown in Fig. 1(b). The PHR sensor was placed at the centre between

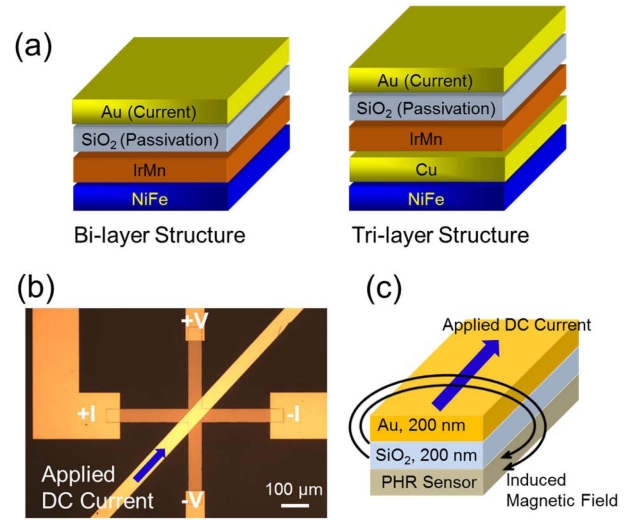


Fig. 1. (Color online) (a) Schematic view of bilayer and trilayer structures, (b) microscopic image of PHR, which represent the PHR voltage between the electrodes of +V and –V, when the driving current flows between the electrodes of +I and –I, and (c) schematic representation of the magnetic field on the PHR sensor produced from the measured current.

two Helmholtz coil systems, for the generation of a uniform magnetic field. A 1 mA current was applied to the PHE sensor, using a current source (Keithley 6220, USA). The DC current applied to the measuring current line (diagonally to the line) was from a source meter (Keithley 2400, USA). The change in output voltage of the PHR sensor was measured, using a Nanovoltmeter (Keithley 2182A, USA).

3. Results and Discussion

3.1. Characterization of sensor

Fig. 2 shows the PHR voltage (V_o) profiles as a function of the applied field (H) in the range of ± 200 Oe of the PHR sensors, based on the bilayer (black color curve), and trilayer (red color curve) structures. The comparison shows that (i) the PHR voltage peak of the sensor by means of the trilayer structure, at about $107\ \mu\text{V}$, is nearly similar to that of the bilayer structure ($121\ \mu\text{V}$); and (ii) the field at the peak of the PHR voltage profile of the sensor by means of the trilayer structure, of about 30 Oe, is 5.5 times larger than that of the bilayer structure (~ 165 Oe). This suggests that the field sensitivity ($S = \Delta V_o / \Delta H$, the slope of the linear part, as shown in Fig. 2) of the sensor by means of the trilayer structure is high. The calculated sensitivity (S) values of the trilayer and bilayer structures are 11.8 and $1.6\ \mu\text{V/Oe}$, respectively. These values support the conclusion that the field sensitivity of

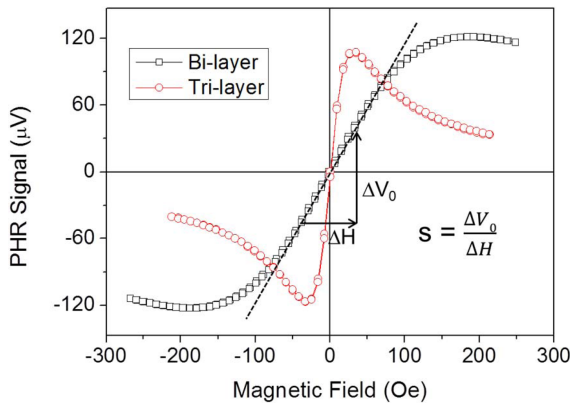


Fig. 2. (Color online) The output voltage versus magnetic-field characteristic curves of the PHR sensor of bilayer and trilayer structures.

the trilayer structure is higher, with respect to the bilayer structure, by a factor of 7.3 times.

3.2. Thermal drift measurement of the PHR sensor

Before proceeding to perform the current monitoring experiments, we perform thermal drift (internal heating of sensor due to driving current) experiments, to determine the signal output stability. Fig. 3 shows the change of PHR signal with time, under 0.1, 0.5, 1 and 2 mA driving current for the bilayer structure. By means of the PHR sensor, no considerable thermal drift was observed in the signals resulted from 0.1, 0.5, 1 and 2 mA current. Therefore, the PHR sensor provides stability in the signal output, for long-term performance of the current monitoring experiments.

3.3. Current monitoring

Fig. 4 shows the response curve of the PHR current

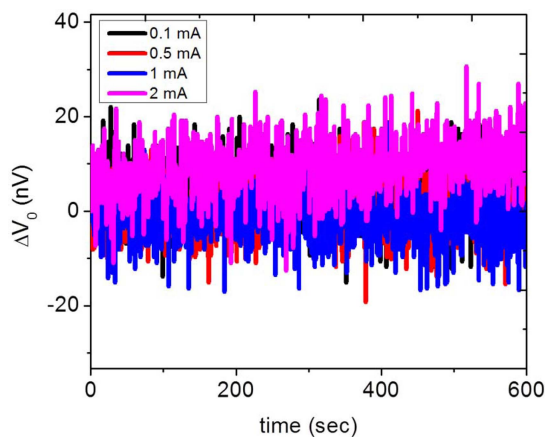


Fig. 3. (Color online) Thermal drift in output voltage of the bilayer PHR sensor, under various driving current.

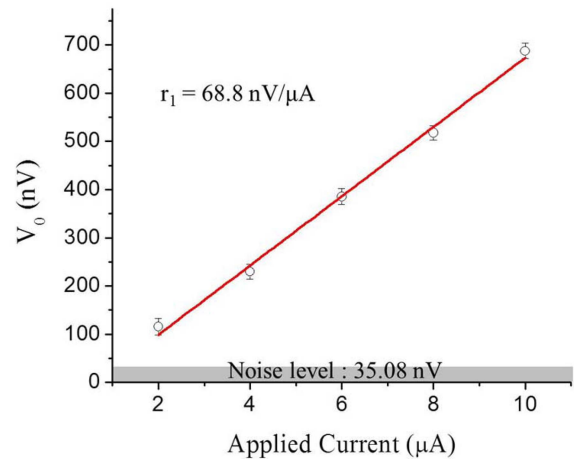


Fig. 4. (Color online) Characteristic curve of the PHR current sensor, using bilayer structure.

sensor using the bilayer structure. As the applied current increases to 10 μA , the output voltage of sensor also increases to 687.87 nV. The sensor output voltage linearly increases with the DC current. The slope (r_1) of this curve is 68.8 nV/ μA . This means that a change of 1 nV output voltage is equal to applying a DC current of 14.5 nA. However, the noise level of PHR output voltage is 35.08 nV. Therefore, the resolution of DC current using the bilayer structured PHR sensor is $35.08 \text{ nV}/(68.8 \text{ nV}/\mu\text{A}) = 0.51 \mu\text{A}$.

The response curve of the trilayer structure is shown in Fig. 5. The sensor output voltage linearly increases with the DC current, as in the bilayer structure. As the applied current increases to 500 nA, the output voltage also increases to 371 nV. The slope (r_2) of this curve is 0.74 nV/nA. This means that a change of 1 nV output voltage is equal to applying a DC current of 1.35 nA. However, the noise level of the output voltage is 40.40 nV. As a

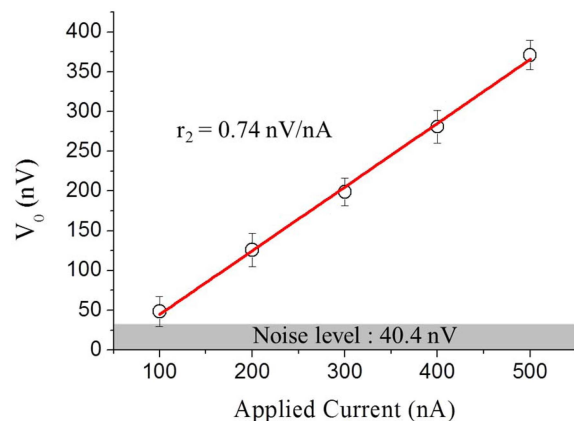


Fig. 5. (Color online) Characteristic curve of the PHR current sensor, using trilayer structure.

result, the resolution of DC current using the trilayer structure is $40.40 \text{ nV}/(0.74 \text{ nV/nA}) = 54 \text{ nA}$. Therefore, in comparison with the bilayer structured PHR, the trilayer structured PHR shows a resolution of about 50 nA, which is almost 10 times less than for the bilayer structure. As discussed in an earlier section in relation to Fig. 2, the PHR sensor with trilayer structure is more sensitive than the PHR sensor with bilayer structure, and the results of current monitoring also show good agreement with these results.

4. Conclusions

In this study, a new application of the PHR sensor to monitor current has been investigated. The output voltages of both bilayer and trilayer PHR structures increase with an applied current, and show good linearity. The minimum detection limit of the PHR current sensor with bilayer and trilayer PHR structures showed $0.51 \mu\text{A}$ and 54 nA respectively. Therefore, between the bilayer and trilayer PHR sensors, the results show that the PHR sensor with trilayer structure is the best choice, to detect ultra low current of the few tens nanoampere range.

Acknowledgement

The authors are thankful to Professor Kim CheolGi, Director of NanoBioEngineering and SpinTronics, Chungnam National University, Korea, for providing the research facilities.

References

- [1] J. A. Ferreira, W. A. Cronje, and W. A. Relihan, *IEEE Trans. Power Electron.* **10**, 32 (1995).
- [2] M. Shafiq, G. A. Hussain, L. Kutt, and M. Lehtonen, *Measurement* **49**, 126 (2014).
- [3] Z. P. Wang, Q. B. Li, Y. Qi, Z. J. Huang, and J. H. Shi, *Opt. Laser. Technol.* **38**, 87 (2006).
- [4] M. Banjevic, B. Furrer, M. Blagojevic, and R. S. Popovic, *Sensor Actuat. A-Phys.* **178**, 64 (2012).
- [5] S. J. Petricevic, Z. Stojkovic, and J. B. Radunovic, *IEEE Instrum. Meas.* **55**, 923 (2006).
- [6] S. Ziegler, R. C. Woodward, H. H. Iu, and Lawrence J. Borle, *IEEE Sens. J.* **9**, 354 (2009).
- [7] S. H. Cheng and S. F. Lin, *Sensor Actuat. A-Phys.* **193**, 112 (2013).
- [8] R. S. Popovic, Z. Randjelovic, and D. Manic, *Sensor Actuat. A-Phys.* **91**, 46 (2001).
- [9] J. Zubia, L. Casado, G. Aldabaldetrekua, A. Montero, E. Zubia, and G. Durana, *Sensors* **13**, 13584 (2013).
- [10] A. R., C. Reig, M. D. Cubells-Beltran, J. B. Roldan, D. Ramirez, S. Cardoso, and P. P. Freitas, *Solid State Electron.* **54**, 1606 (2010).
- [11] P. Mlejnek, M. Vopalensky, and P. Ripka, *Sensor Actuat. A-Phys.* **141**, 649 (2008).
- [12] S. Oh, M. Jadhav, J. Lim, V. Reddy, and C. G. Kim, *Biosens. Bioelectron.* **41**, 758 (2013).
- [13] B. Sinha, T. S. Ramulu, K. W. Kim, R. Venu, J. J. Lee, and C. G. Kim, *Biosens. Bioelectron.* DOI No: 10.1016/j.bios.2014.03.021 (2014).
- [14] B. Sinha, T. Q. Hung, T. S. Ramulu, S. Oh, and K. Kim, *J. Appl. Phys.* **113**, 063903 (2013).
- [15] H. Kim, V. Reddy, K. W. Kim, I. Jeong, X. H. Hu, and C. G. Kim, *J. Magn.* **19**, 1 (2014).